REPORT DOCUMENTATION PAGE

Form Approved OMB NO. 0704-0188

The public reporting burden for this collection of information is estimated to average 1 hour per response, including the time for reviewing instructions, searching existing data sources, gathering and maintaining the data needed, and completing and reviewing the collection of information. Send comments regarding this burden estimate or any other aspect of this collection of information, including suggesstions for reducing this burden, to Washington Headquarters Services, Directorate for Information Operations and Reports, 1215 Jefferson Davis Highway, Suite 1204, Arlington VA, 22202-4302. Respondents should be aware that notwithstanding any other provision of law, no person shall be subject to any oenalty for failing to comply with a collection of information if it does not display a currently valid OMB control number.
PLEASE DO NOT RETURN YOUR FORM TO THE ABOVE ADDRESS.

1. REPORT DATE (DD-MM-YYYY)	2. REPORT TYPE	3. DATES COVERED (From - To)
28-03-2013	Final Report	5-Jan-2012 - 4-Jan-2013

4. TITLE AND SUBTITLE
Precision Control and Randomized Benchmarking of a 12-us Class Superconducting Qubit

5a. CONTRACT NUMBER
W911NF-12-1-0036

5b. GRANT NUMBER

5c. PROGRAM ELEMENT NUMBER

6. AUTHORS
Terry P. Orlando and William D. Oliver

5d. PROJECT NUMBER

5e. TASK NUMBER

5f. WORK UNIT NUMBER

7. PERFORMING ORGANIZATION NAMES AND ADDRESSES
Massachusetts Institute of Technology (MIT)
77 Massachusetts Ave.
NE18-901
Cambridge, MA 02139 -4307

8. PERFORMING ORGANIZATION REPORT NUMBER

9. SPONSORING/MONITORING AGENCY NAME(S) AND ADDRESS(ES)
U.S. Army Research Office
P.O. Box 12211
Research Triangle Park, NC 27709-2211

10. SPONSOR/MONITOR'S ACRONYM(S)
ARO

11. SPONSOR/MONITOR'S REPORT NUMBER(S)
60716-PH-QC.5

12. DISTRIBUTION AVAILIBILITY STATEMENT
Approved for Public Release; Distribution Unlimited

13. SUPPLEMENTARY NOTES
The views, opinions and/or findings contained in this report are those of the author(s) and should not contrued as an official Department of the Army position, policy or decision, unless so designated by other documentation.

14. ABSTRACT
This work addresses the randomized benchmarking (RBM) of a long-lived superconducting flux qubit (T1 = 12 us, T2E = 23 us). Our aim is to use this long-lived qubit to develop the precision calibration and control capabilities necessary to measure a RBM fidelity at the 99.9% level. During this reporting period, we have developed a calibration technique that images the envelope of the control pulse that arrives at the qubit. This accounts for quadrature pulse distortion within the dilution refrigerator. Using this technique and pulse predistortion, we

15. SUBJECT TERMS
qubit, calibration, randomized benchmarking, coherence, noise spectroscopy

16. SECURITY CLASSIFICATION OF:			17. LIMITATION OF ABSTRACT	15. NUMBER OF PAGES	19a. NAME OF RESPONSIBLE PERSON
a. REPORT	b. ABSTRACT	c. THIS PAGE			Terry Orlando
UU	UU	UU	UU		19b. TELEPHONE NUMBER 617-253-5888

Report Title

Precision Control and Randomized Benchmarking of a 12-us Class Superconducting Qubit

ABSTRACT

This work addresses the randomized benchmarking (RBM) of a long-lived superconducting flux qubit (T1 = 12 us, T2E = 23 us). Our aim is to use this long-lived qubit to develop the precision calibration and control capabilities necessary to measure a RBM fidelity at the 99.9% level. During this reporting period, we have developed a calibration technique that images the envelope of the control pulse that arrives at the qubit. This accounts for quadrature pulse distortion within the dilution refrigerator. Using this technique and pulse predistortion, we achieved 99.814% RBM fidelity. In addition, we applied these calibrated pulses to dynamical decoupling and coherence studies of our superconducting qubits.

Enter List of papers submitted or published that acknowledge ARO support from the start of the project to the date of this printing. List the papers, including journal references, in the following categories:

(a) Papers published in peer-reviewed journals (N/A for none)

Received		Paper
03/28/2013	4.00	Simon Gustavsson, Olger Zwier, Jonas Bylander, Fei Yan, Fumiki Yoshihara, Yasunobu Nakamura, Terry P. Orlando, William D. Oliver. Improving Quantum Gate Fidelities by Using a Qubit to Measure Microwave Pulse Distortions, Physical Review Letters, (01 2013): 0. doi: 10.1103/PhysRevLett.110.040502
08/16/2012	1.00	Fei Yan, Simon Gustavsson, Jonas Bylander, Fumiki Yoshihara, Yasunobu Nakamura, Terry Orlando, William Oliver. Dynamical Decoupling and Dephasing in Interacting Two-Level Systems, Physical Review Letters, (07 2012): 0. doi: 10.1103/PhysRevLett.109.010502
08/16/2012	2.00	David Cory, Jonas Bylander, Fei Yan, Simon Gustavsson, Fumiki Yoshihara, Khalil Harrabi, Terry Orlando, Yasunobu Nakamura, Jaw-Shen Tsai, William Oliver. Spectroscopy of low-frequency noise and its temperature dependence in a superconducting qubit, Physical Review B, (05 2012): 0. doi: 10.1103/PhysRevB.85.174521
08/16/2012	3.00	S. Gustavsson, J. Bylander, F. Yan, P. Forn-Díaz, V. Bolkhovsky, D. Braje, G. Fitch, K. Harrabi, W. Oliver, D. Lennon, J. Miloshi, P. Murphy, R. Slattery, S. Spector, B. Turek, T. Weir, P. Welander, F. Yoshihara, D. Cory, Y. Nakamura, T. Orlando. Driven Dynamics and Rotary Echo of a Qubit Tunably Coupled to a Harmonic Oscillator, Physical Review Letters, (04 2012): 0. doi: 10.1103/PhysRevLett.108.170503
TOTAL:	**4**	

Number of Papers published in peer-reviewed journals:

(b) Papers published in non-peer-reviewed journals (N/A for none)

Received Paper

TOTAL:

Number of Papers published in non peer-reviewed journals:

(c) Presentations

i. Conference: 2012 APS March meeting, F. Yan, J. Bylander, S. Gustavsson, F. Yoshihara, D.G. Cory, Y. Nakamura, W.D. Oliver, "T1rho experiment as a noise spectrum analyzer"

ii. Conference: 2012 APS March meeting, J. Bylander, S. Gustavsson, F. Yan, K. Harrabi, F. Yoshihara, Y. Nakamura, J.-S. Tsai, D.G. Cory, T.P. Orlando, W.D. Oliver,"T1rho experiment as a noise spectrum analyzer"

iii. Conference: 2012 APS March meeting, S. Gustavsson, J. Bylander, F. Yan, P. Forn-Diaz, V. Bolkhovsky, D. Braje, S. Spector, B. Turek, P.B. Welander, F. Yoshihara, D.G. Cory, Y. Nakamura, W.D. Oliver, "Driven dynamics of a qubit tunably coupled to a harmonic oscillator"

iv. Seminar: RWTH Aachen, Germany, March 20, 2012, S. Gustavsson, "Noise spectroscopy through dynamical decoupling with a superconducting flux qubit"

v. Seminar: ETH Zurich, Switzerland, March 23, 2012, S. Gustavsson, "Noise spectroscopy through dynamical decoupling with a superconducting flux qubit"

vi. Conference: Quantum Physics of Phase, Royal Institute of Technology (KTH), Stockholm, Sweden, April 23, 2012, S. Gustavsson, "Noise characterization and mitigation by dynamical decoupling with a superconducting flux qubit"

vii. Seminar: U. Groningen, The Netherlands, July 5, 2012, S. Gustavsson, "Noise spectroscopy through dynamical decoupling with a superconducting flux qubit"

viii. Seminar: Chalmers University of Technology, Gothenburg, Sweden, September 25, 2012, S. Gustavsson, "Dynamical decoupling with superconducting qubits"

ix. Seminar: Auburn University, November 1, 2012, W.D. Oliver, "Superconducting qubits"

Number of Presentations: 9.00

Non Peer-Reviewed Conference Proceeding publications (other than abstracts):

Received Paper

TOTAL:

Number of Non Peer-Reviewed Conference Proceeding publications (other than abstracts):

Peer-Reviewed Conference Proceeding publications (other than abstracts):

Received Paper

TOTAL:

Number of Peer-Reviewed Conference Proceeding publications (other than abstracts):

(d) Manuscripts

Received Paper

TOTAL:

Number of Manuscripts:

Books

Received Paper

TOTAL:

Patents Submitted

Patents Awarded

Awards

Graduate Students

NAME	PERCENT_SUPPORTED
FTE Equivalent:	
Total Number:	

Names of Post Doctorates

NAME	PERCENT_SUPPORTED
Simon Gustavsson	0.75
FTE Equivalent:	**0.75**
Total Number:	**1**

Names of Faculty Supported

NAME	PERCENT_SUPPORTED	National Academy Member
Terry P. Orlando	0.05	
FTE Equivalent:	**0.05**	
Total Number:	**1**	

Names of Under Graduate students supported

NAME	PERCENT_SUPPORTED
FTE Equivalent:	
Total Number:	

Student Metrics

This section only applies to graduating undergraduates supported by this agreement in this reporting period

The number of undergraduates funded by this agreement who graduated during this period:	0.00
The number of undergraduates funded by this agreement who graduated during this period with a degree in science, mathematics, engineering, or technology fields:.....	0.00
The number of undergraduates funded by your agreement who graduated during this period and will continue to pursue a graduate or Ph.D. degree in science, mathematics, engineering, or technology fields:.....	0.00
Number of graduating undergraduates who achieved a 3.5 GPA to 4.0 (4.0 max scale):	0.00
Number of graduating undergraduates funded by a DoD funded Center of Excellence grant for Education, Research and Engineering:	0.00
The number of undergraduates funded by your agreement who graduated during this period and intend to work for the Department of Defense	0.00
The number of undergraduates funded by your agreement who graduated during this period and will receive scholarships or fellowships for further studies in science, mathematics, engineering or technology fields:	0.00

Names of Personnel receiving masters degrees

NAME
Total Number:

Names of personnel receiving PHDs

NAME
Total Number:

Names of other research staff

NAME	PERCENT_SUPPORTED
William D. Oliver	0.00
FTE Equivalent:	**0.00**
Total Number:	**1**

Sub Contractors (DD882)

Inventions (DD882)

Scientific Progress

Technology Transfer

Precision Control and Randomized Benchmarking of a 12-us Class Superconducting Qubit

Executive Summary

Superconducting qubits are solid-state artificial atoms, comprising lithographically defined Josephson tunnel junctions and superconducting interconnects. When cooled to milli-Kelvin temperatures, these superconducting circuits exhibit quantized states of flux, charge, or junction phase depending on design parameters. Such superconducting artificial atoms have already proven a useful vehicle for advancing the scientific community's general understanding of coherence, quantum mechanics, and atomic physics, particularly in regimes not easily accessible with natural atoms and molecules. Their potential for lithographic scalability, compatibility with microwave control, and operability at nanosecond time scales make superconducting qubits a promising candidate for quantum information science and technology applications.

The primary focus of this program was to develop the calibration techniques required to eliminate pulse errors. By eliminating these errors, we aimed to achieve a randomized benchmarking single-qubit fidelity of 99.9%. The pulse errors we addressed, in particular, are those which occur inside the dilution refrigerator.

To image the pulse infidelity, we used the qubit as an oscilloscope to "visualize" the pulse shape that actually arrived at the qubit. Ideally, we want a Gaussian pulse shape to arrive at the qubit. Outside the dilution refrigerator, we directly measure the transfer function with an oscilloscope and use it then predistort the pulse to ensure that a Gaussian pulse enters the refrigerator. However, inside the refrigerator, impedance mismatch and frequency-dependent loss serves to distort the pulse. We used the qubit itself to image the pulse and, thereby, infer the transfer function in the refrigerator. We then predistorted the pulse to ensure it arrived at the qubit as a Gaussian. During this period of performance, we targeted errors in the quadrature (Q) microwave component of our pulses. In a future program, we would like to extend this approach to in-phase (I) errors.

Using these improved pulses, we achieved 99.8%, more than a 30% improvement compared with before the start of this program. This resulted in a publication in PRL [1].

A second focus of this program was to demonstrate improved quantum control of our qubit using these improved pulses, and this line of work led to three publications during this period. In one work, we used the pulses to implement a "rotary echo," the driven-evolution version of the Hahn spin-echo [2]. In another publication, we showed that we could use dynamical decoupling pulse sequences to improve phase coherence in coupled two-level-systems (in this case, a qubit and an impurity) [3]. Finally, we used microwave pulses to enable single-shot, low-frequency noise measurements in the milliHertz to 100 Hz frequency band [4].

Introduction

Background on the persistent-current qubit

In this work, we used a superconducting persistent-current (PC) qubit [5,6]. The PC flux qubit comprises a superconducting loop interrupted by four Josephson junctions (Fig.1A). When biased with a static magnetic flux $f_{dc} \sim \Phi_0/2$, where Φ_0 is the superconducting flux quantum, the system assumes a double-well potential profile. The diabatic ground state of the left (right) well corresponds to a persistent current I_q with clockwise (counterclockwise) circulation. The two diabatic energy levels have an energy separation $\varepsilon = 2 I_q \delta f_{dc}$ linear in the flux detuning $\delta f_{dc} = f_{dc} - \Phi_0/2$. Higher-excited states of the double-well potential exist, although we focus on the lowest two states here.

The two-level system Hamiltonian for the lowest-two states is: $\boldsymbol{H^{TLS} = -1/2\,[\varepsilon\sigma_z + \Delta\sigma_x]}$. At detuning δf_{dc}=0, the double-well potential is symmetric and the diabatic-state energies are degenerate. At this ``degeneracy point,'' $\varepsilon = 0$ and resonant tunneling opens an avoided level crossing of energy Δ. Here, the qubit states are σ_x eigenstates, corresponding to symmetric and anti-symmetric combinations of diabatic circulating-current states. At this point, the qubit is first-order insensitive to flux noise (the energy level spacing is independent of flux around this point), but maximally sensitive to charge and critical current noise. Detuning the flux away from this point tilts the double well, allowing us to tune the eigenstates and eigenenergies of the artificial atom.

Far from the degeneracy point, $\varepsilon >> \Delta$, the qubit states are approximately σ_z eigenstates, i.e., the diabatic states with well-defined circulating current. Here, the qubit is maximally sensitive to flux noise with reduced sensitivity to charge and critical current noise. The qubit is read out using a hysteretic DC SQUID (superconducting quantum interference device), a sensitive magnetometer that distinguishes the flux generated by circulating current states.

Coherence characterization of the flux qubit (previous AOR/LPS program) [7]

In work funded by the ARO and LPS, previous to this program, we characterized the coherence of the long-lived qubit used in the present program. We first briefly review these results to introduce the qubit. Figs. 1A-D present an SEM of the PC qubit used in these measurements, along with its measured relaxation (T_1=12 us), spin-echo (T_{2E}=23 us), Ramsey (T_2*=2.5 us), and Rabi (T_{Rabi}=13 us) decay traces when biased at the flux-insensitive bias point (degeneracy point). At this bias, the spin echo is efficient ($T_{2E} \sim 2T$), although the inhomogenous Ramsey is not ($T_2^* < T_1$). Away from this bias point, the qubit becomes more sensitive to flux noise.

To understand why the Ramsey time T_2* was less than the spin-echo time T_{2E}, we considered the filter function picture of the Carr-Purcell-Meiboom-Gill (CPMG) pulse sequence (Fig. 1E). The filter function is essentially the Fourier transform of the free-evolution period between pi-pulses. For a Ramsey sequence (N=0), the free-evolution period is a “box car” rectangle, which transforms to a sinc function in frequency (Fig. 1F, N=0). The spin-echo comprises two box cars, with one period acquiring a negative sign due to the single pi-pulse which flips the Bloch vector 180 degrees about the driving field. Its Fourier transform is a sinc-like function offset from zero frequency (Fig. 1F, N=1). As more pi-pulses are added, the filter function peaks at higher and higher frequencies. For noise power spectra that decrease with frequency, this is a good situation: more pi-pulses lead to lower integrated noise power and therefore longer coherence times.

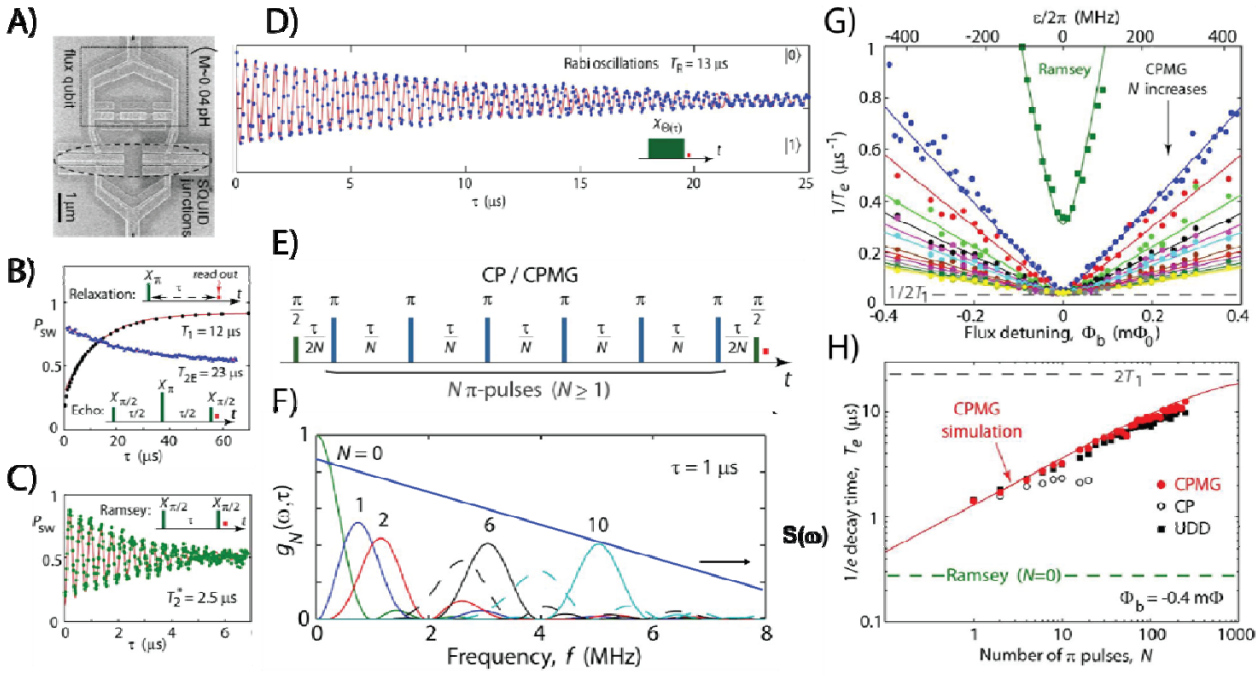

Fig. 1: Coherence characterization of a long-lived persistent-current flux qubit used in this work [7]. A) SEM of the persistent-current flux qubit. B) Relaxation time T_1 = 11.7 us and spin-echo time T_{2E} = 23 us; C) Ramsey interferometry yielding an inhomogeneous coherence time T_2* = 2.5 us; and D) Rabi oscillations with decay time T_{Rabi} = 13 us, all B-D measured at the flux-insensitive degeneracy point. E) Carr-Purcell-Meiboom-Gill (CPMG) pulse sequence contains N pi-pulses that are aligned with (CP) or in quadrature to (CPMG) the pi/2 pulses. F) The pulse sequence in time corresponds to a filter function in the frequency domain that acts to color the noise. Increasing the pulse number moves the filter function to higher frequency and, for noise power spectra that decrease in magnitude with frequency, leads to longer coherence times. G) Measurement of the 1/e-decay rate as a function of the qubit flux detuning Φ_b. First-order flux insensitive point at Φ_b = 0. Away from this point, flux noise increases, increasing the decay rate. Increasing the number of CPMG pulses drives down the decoherence rate (improves decoherence time). H) 1/e-decay time as a function of the number of CPMG pulses at Φ_b = -0.4 m□$_0$,where the qubit is sensitive to flux noise. Increasing the number of pulses improves the decay time out to 250 pulses. Uhrig dynamical decoupling (UDD) is another sequence compared in this work.

Fig. 1G shows the decay rate as a function of flux (quantization axis) and number N of pi-pulses. At the degeneracy point (Φ_b = 0), the Ramsey decay rate corresponds to 1 / 2.5 us, while the decay rate for spin-echo (N=1) and all CPMG pulses (N>1) is efficient, that is, 1 / 2T_1. Note that although flux noise dominates, residual charge and critical current noise are the reason the Ramsey decay rate 1/ T_2* is greater than the relaxation rate 1/ T_1. It is inconsistent with second-order flux noise in this device. Away from Φ_b = 0, the flux noise sensitivity increases, and the decay rates generally increase. Increasing the number of pi-pulses reduces the decay rate (increases coherence times). In Figure 1G, the coherence time is shown to improve with pulse number out to several hundred pulses, in agreement with simulation.

Summary of work performed during the present funding period

Pulse calibration and randomized benchmarking single-qubit fidelity F = 99.8% [1]

In Fig. 2A, the desired Gaussian pulse that we attempt to apply to the device is distorted by the frequency-domain transfer function $H = H_{ext}\, H_{int}$ due to impedance mismatch, mixer imperfections, etc. If we know H, we can invert it (H^{-1}) to predistort the starting pulse X such that we obtain the desired pulse at the output, $Y = H(H^{-1}\, X) = X$. The transfer function H_{ext} corresponds to those distortions that occur outside the dilution refrigerator, which can be found by measuring the impulse response of the external system on an oscilloscope. However, there are also distortions arising from imperfections inside the refrigerator which cannot be calibrated using an oscilloscope. To address this, we developed a scheme whereby the qubit itself measures the impulse response. This approach targets quadrature errors only (note: in our new proposal, we will target in-phase errors). The resulting improvement in the randomized benchmarking decay (Fig. 2B), and in the corresponding error rate versus pulse width (Fig.2C) indicates that imperfections inside the refrigerator matter, and that using the qubit to measure their transfer function leads to a reduced error rate. Using this approach, we obtained a single-qubit randomized benchmarking fidelity 99.8% for a 4-ns wide pulse.

Dynamical decoupling of coupled coherent systems and the rotary echo [2,3]

We applied the advanced pulses to address coherence mitigation in two experiments. The first is the dynamical protection of an entangled state of the qubit and a two-level system (Fig. 2D) in the space spanned by the SWAP operation. We developed a pulse sequence that refocuses the coupled-system with N refocusing pulses (Fig. 2E), extending the coherence time of the SWAP oscillations (Fig. 2F) with the number of pulses (Fig. 2G). This is essentially a demonstration of dynamical decoupling with coupled qubits [2].

The second example is “rotary echo” (Fig. 2H), the driven-evolution counterpart to spin-echo [3]. With spin echo, a pi-pulse quickly rotates the Bloch vector by 180 degrees about the driving axis, and then the refocusing occurs during the qubit’s free evolution. In the rotary echo case, the qubit is driven (as in a Rabi oscillation), and it is the driving field that is phase shifted by 180 degrees. In this case, refocusing occurs during the driven evolution. Fig. 2I compares the decay traces of a conventional Rabi driving experiment with a rotary echo experiment for a particular Rabi frequency (driving amplitude), and Fig. 2J shows the dependence of the decay time on driving field. In all cases, the rotary echo outperforms conventional Rabi flopping.

In performing these measurements, we identified a new noise source that may arise in qubits coupled to harmonic oscillators. In this case, there are two driving channels: one is the desired direct driving of the qubit, and the other is a secondary drive as mediated by the oscillator (in our case, the readout SQUID) with altered amplitude and phase. Fig. 2K shows one consequence of this effect, in which despite a *constant* driving amplitude, the observed Rabi frequency changes with SQUID bias current (oscillator parameters). That means that current noise (fluctuating oscillator parameters) causes Rabi-frequency fluctuations. It is this driving-field amplitude noise that the rotary echo corrects in our experiment.

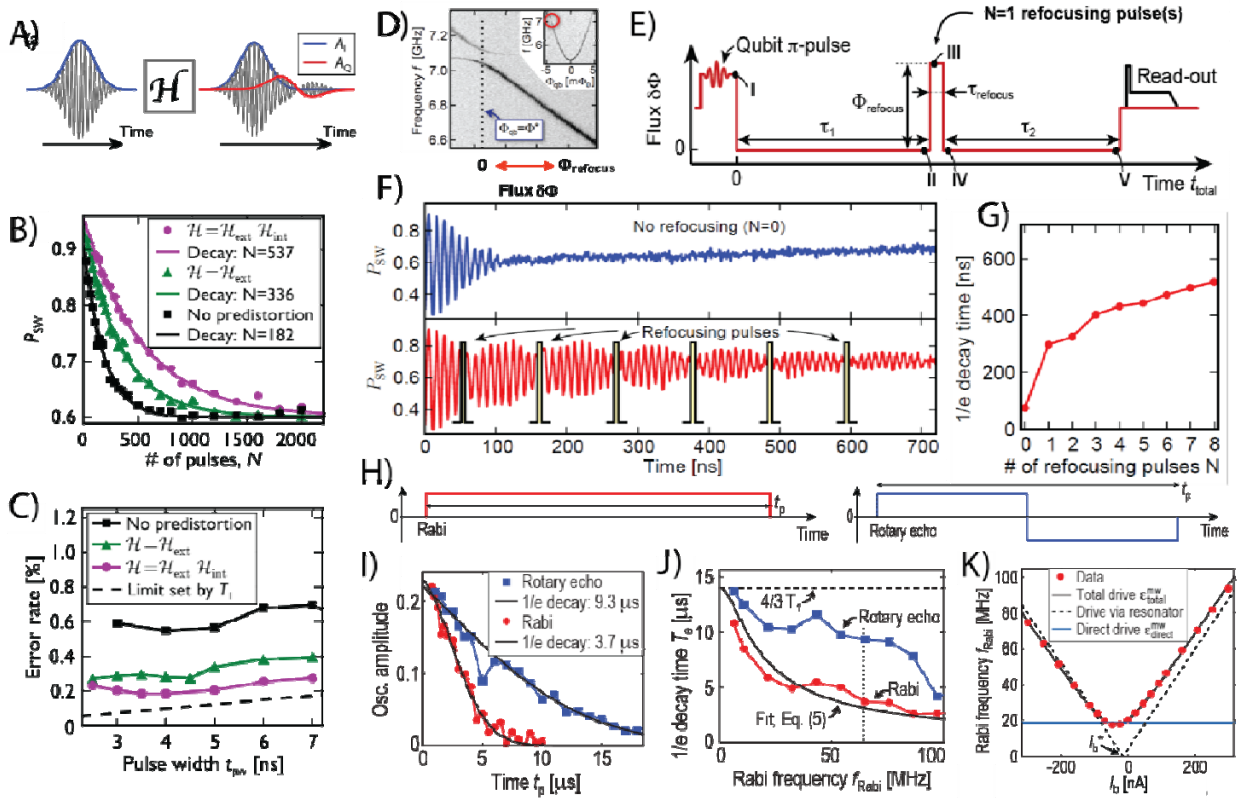

Fig. 2: Pulse calibration and examples of advanced dynamical decoupling [13 ,14]. A) Desired Gaussian pulse becomes distorted by the transfer function *H* due to imperfections in pulse generation and transmission. Predistorting with H^{-1} can correct for these errors. B) Decay traces for cases of no predistortion, predistortion accounting only for effects external to the refrigerator, and predistortion using a transfer function measured by the qubit which incorporates distortions internal to the refrigerator. C) Randomized benchmarking error rate for these cases as function of pulse width. F = 99.85% is achieved with a 4-ns pulse width. D) Spectrum of qubit coupled to a two-level system (TLS). E) Dynamical decoupling sequence that mitigates low-frequency errors in the SWAP operation between the qubit and the TLS. F) SWAP operation in the cases of N=0 refocusing pulses and N=6 refocusing pulses. G) SWAP decay time versus number N of pulses. H) Conventional Rabi pulse and its corresponding rotary-echo pulse, which applies a 180-degree phase shift to the drive. I) Oscillation decay trace for the Rabi (red) and rotary echo (blue). J) Decay times versus Rabi frequency (driving amplitude) for both Rabi and rotary echo. Rotary echo generally has a longer decay time. K) The readout SQUID, an oscillator, is a second channel for the driving field to reach the qubit, modifying its Rabi frequency, shown as a function of the SQUID bias.

Low-frequency noise characterization via repeated Ramsey interferometry [4]

In the present work, we used our advanced pulses to measure the low-frequency noise spectrum in the 0.1 mHz – 100 Hz regime using a Ramsey interferometry technique [4]. Low frequency fluctuations in ε and Δ translate into fluctuations in the Ramsey fringes, which we measured and analyzed to extract the noise power spectral density (PSD). Amazingly, the 1/f nature is consistent with our previous work (previously funded by ARO/LPS) across 10 decades in frequency. If we extend the low-frequency flux noise out to the qubit frequency Δ = 5.4 GHz, it matches the strength required for T_1 relaxation noise (the flux noise couples transversally only at this frequency). This suggests that the low-frequency flux

noise responsible for dephasing may be the same mechanism for relaxation, motivating us to measure the noise at higher frequencies (future work).

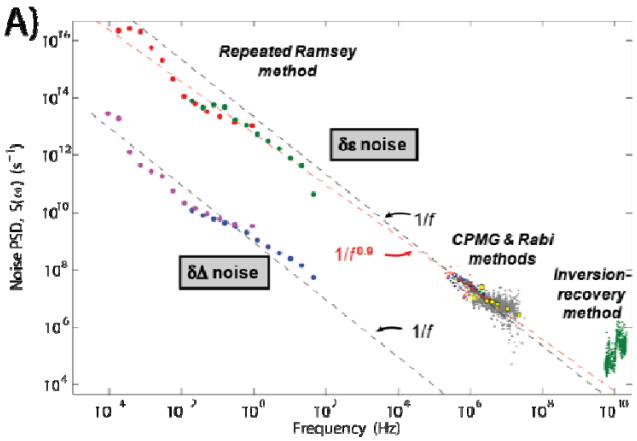

Fig. 3: Characterizing low frequency noise using advanced pulse sequencing techniques [4]. A) Noise power spectral density (PSD) for both σ_x ($\delta\Delta$) and σ_z ($\delta\varepsilon$) noise. In the present work, we used the advanced pulses to measure low-frequency noise (portion of plot at frequencies f< 100 Hz) using a repeated Ramsey interferometry technique [4]. The other portions of this plot were performed under a previous ARO/LPS program [7].
.

[1] S. Gustavsson, O. Zwier, J. Bylander, F. Yan, F. Yoshihara, Y. Nakamura, T.P. Orlando, W.D. Oliver, Improving quantum gate fidelities by using a qubit to measure microwave pulse distortions, PRL 110, 040502 (2013).

[2] S. Gustavsson, J. Bylander, F. Yan, P. Forn-Diaz, V. Bolkhovsky, D. Braje, G. Fitch, K. Harrabi, D. Lennon, J. Miloshi, P. Murphy, R. Slattery, S. Spector, B. Turek, T. Weir, P.B. Welander, F. Yoshihara, D.G. Cory, Y. Nakamura, T.P. Orlando, W.D. Oliver, Driven dynamics and rotary echo of a qubit tunably coupled to a harmonic oscillator, PRL 108, 170503 (2012).

[3] S. Gustavsson, F. Yan, J. Bylander, F. Yoshihara, Y. Nakamura, T.P. Orlando, W.D. Oliver, Dynamical decoupling and dephasing in interacting two-level systems, PRL 109, 010502 (2012).

[4] F. Yan, J. Bylander, S. Gustavsson, F. Yoshihara, K. Harrabi, D.G. Cory, T.P. Orlando, Y. Nakamura, J.-S. Tsai, W.D. Oliver, Spectroscopy of low-frequency noise and its temperature dependence in a superconducting qubit, PRB 85, 174521 (2012).

[5]T.P. Orlando, J.E. Mooij, L. Tian, C.H. van der Wal, L.S. Levitov, S. Lloyd, J.J. Mazo, Superconducting persistent-current qubit, PRB 60, 15398-15413 (1999).

[6] J.E. Mooij, T.P. Orlando, L.S. Levitov, L. Tian, C.H. van der Wal, S. Lloyd, Josephson persistent-current qubit, Science 285, 1036-1039 (1999).

[7] J. Bylander, S. Gustavsson, F. Yan, F. Yoshihara, K. Harrabi, G. Fitch, D.G. Cory, Y. Nakamura, J.S. Tsai, W.D. Oliver, Noise spectroscopy through dynamical decoupling with a superconducting flux qubit, Nature Physics 7, 565-570 (2011).